New Nondestructive Method to Rapidly Detect and Quantify Surface and Bulk Corrosion in Steel with Real-Time Monitoring using Vipulanandan Impedance Corrosion Model

C. Vipulanandan Ph.D., P.E.
Honorable Daniel Wong Endowed Professorship
"**Smart Cement**" Inventor
"**Vipulanandan Rheological Model**"
"**Vipulanandan Failure Model**"
Chief Editor – Advances in Civil Engineering
Director, Center for Innovative Grouting Material and Technology (CIGMAT)
Director, Texas Hurricane Center for Innovative Technology (THC-IT)
Professor of Civil and Environmental Engineering
University of Houston, Houston, Texas 77204-4003

1. Abstract

In this study, carbon steel corrosion was evaluated in salt water solutions using the newly developed non-destructive electrical method which can be easily adopted in the field for real-time monitoring and the results were compared to some standard test methods such as weight loss, corrosion rate and potential difference. The average weight loss in 10% salt solution (accelerated corrosion and also representing the hydraulic fracking fluids) in one year was 1.05% and corrosion rate was 1.54 mm/year, using the ASTM G1 method. Vipulanandan correlation model was used to represent the weight loss versus time relationship. The potential difference between the corroding steel and standard calomel electrode in 1M salt solution reduced from -0.680 V to -0.791 V in two years, a 15% total change. The use of the new nondestructive electrical method was to detect and quantify the surface and bulk corrosion in the field. Tests were performed to first verify the best electrical property that will be highly sensitive and represent the steel corrosion. The findings from this study indicated changes in the newly developed electrical corrosion index for the surface (2D representation) and the resistivity (second order tensor, 3D representation) for the bulk material using the Vipulanandan Impedance Corrosion Model. Corrosion development in 750 mm (30 inches) long steel specimens were studied in the 3.5% salt solution (simulating sea water) for 500 days. The changes in the specimens were monitored at regular intervals using the new two probe method and measuring the impedance-frequency relationship using alternative current up to a frequency of 300 kHz. The surface corrosion was quantified using the new electrical corrosion index parameter, which changed from point to point on the surface of the corroding steel and the change was over 200%. The change in the bulk resistivity along the length of the steel specimen was over 40,000 times (4,000,000%) in 3.5% salt solution compared to the weight loss and reduction in the potential difference. Hence the electrical resistivity for the bulk material and the new corrosion index for the surface corrosion are highly sensing parameters for detecting and quantify the corrosion in the steel.

2. Introduction

Major concerns related to maintenance of bridges, buildings, rail tracks, oil and gas wells, chemical plants, power plants, pipelines and mobile facilities are due to corrosion caused by the service conditions and exposed environments, aging of the facilities, types of usage and composition of the materials. In order to improve the maintenance operations and also extend the service life of bridges, buildings, rail tracks, oil and gas wells, petrochemical plants, pipelines and supporting infrastructures it is very important to detect and quantify corrosion real-time (Vipulanandan et al. 2002-2018, U.S. Patent 2019). Corrosion degrades the material by bio-chemical reactions, stress fatigue degradation, temperature cycles with the exposed environments. In addition to daily encounters with this kind of degradation, corrosion causes oil and gas well failures, fire hazards due to pipeline leakages, plant shutdowns, waste of valuable resources, loss and contamination of product, reduction in productivity and expensive maintenance.

Corrosion of metals alone cost the U.S. economy billions of dollars per year and approximately one-third of these cost could be saved by proper corrosion detection and quantification (Corrosion: Understanding the basics, 2000). NACE has reported that losses due to corrosion are equal to 1 to 5 % of the country's Gross National Product (GNP) which sums ups to several billion dollars. The annual cost of corrosion in the USA oil and gas industry is over $27 billion and globally $60 billion (Papavinasam, 2013).

Steel is the largest volume of metal used in the construction of bridges, buildings, rail tracks, oil and gas wells, pipelines, operating machines, piles and storage facilities. Also, the corrosion of steel will not only affect the exposed surfaces but also the integrity of the bulk material. Corrosion changes have to be quantified point-to-point or section-by-section to better understand the corrosion processes and also to develop mitigation methods. Corrosion of steel or any other material is a bio-chemo-physical-stress-thermo (BCPST) induced parallel and/or series processes (representing the environment and usage) and the corrosion and degradation are very much influence by the maintenance of the facilities. Although there are hundreds of standard testing methods such as visual inspection, potential difference, weight change, thickness change and acoustic monitoring used to detect and quantify corrosion these methods have many limitations including field applications. Also, the current testing methods cannot quantify the corrosion based on the material property degradation from section to section in various directions and also separate the surface corrosion from the bulk corrosion. Hence, understanding the rate of steel property degradation due to corrosion is essential to designing the steel-based facilities to avoid excessive deflection and failure (Decker et al. 2008). Corrosion occurs in unprotected steel structures in any location and varies in intensity depending on the local variables related to BCPST (Krebs 2003; Hilbert 2006; Chiew et al. 2011). Accelerated Low Water Corrosion (ALWC) is defined as the localized and aggressive corrosion phenomenon that typically occurs at or below low-water level and is associated with microbially induced corrosion. ALWC corrosion rates are typically 0.5 mm/side/year averaged over time to the point of complete perforation of steel plate. (Cheung et al. 1994; Davis 2000; Kumar, et al. 2002; Zhao et al. 2007; Decker et al. 2008; Vipulanandan et al. 2012). Marine environments normally encompass several

exposure zones of differing aggressively and the corrosion performances of marine structures in these zones require separate considerations. These zones with the high tide and microbiological activities will contribute to the accelerated low water corrosion (ALWC). Accelerated low water corrosion (AWLC) usually occurs between meaning low water springs (MLWS) and low tide. Occurrences of ALWC have been noted in the literature as far back as the first half of the 20th century.

Within the past 20 to 30 years, there has been growing awareness of an accelerated form of corrosion concentrated around the low-water mark of maritime structures. This Accelerated Low Water Corrosion, or ALWC, is a rapid pitting form of microbial induced corrosion (MIC) that occurs more rapidly than others previously identified (Cheung et al. 1994; Jothilakshmi et al. 2013). The most common variety of ALWC occurs as a horizontal band around low water, but it can be found occasionally in patches and extends down to bed level.

Historical Theories of Corrosion

One of essential contribution was made by Faraday (1791- 1867) who established a measurable relationship between chemical activity and electrical current (Kerbs, 2003; Masadeh 2005; Hamdy et al. 2006; Zaki 2006). Ideas on corrosion control began to be produced at the starting of the 19th century (Whitney, 1903). Evans (1923) provided a modern-day understanding of the reasons and also control of corrosion based upon his classic electrochemical theory. Forrest, Roetheli and Brown (1931), revealed that rust layers changed the protective nature in accordance with the speed of attack of oxygen to the area, the exact same principle was discovered to function in statistical experiments with oxygen-nitrogen mixtures completed by Mears throughout his function in the writer's research laboratory (Mears et al. 1935). These suggested that oxygen can depress the likelihood of corrosion beginning within a certain region, even though, where after the corrosion has set in, oxygen accelerates the corrosion velocity , this differentiation between corrosion velocity and corrosion probability has served to get rid of a number of the obvious contradictions of earlier researchers. Now there are many testing standards for corrosion developed by professional societies.

Current Methods of Corrosion Detection and Quantification

Corrosion changes the material properties of the metal - decreasing its strength, changing its structure. Hence it is important to be able to detect and evaluate the extent of corrosion of the metal surface. There are many methods that are employed to evaluate corrosion, visual inspection, weight loss measurements, material composition variation, and studies of the compositions of the deposition material using X-ray diffraction (XRD) measurements. Summary of some of the current inspection, deterioration and monitoring methods are as follows:

a) **Visual Inspection (ASTM G4, NACE Standard RP0497):** This can be done only if there is physical access to the corroded material. The inspection can only identify surface corrosion, including general corrosion, pitting corrosion, crevice

corrosion, weld and heat affected zone corrosion, erosion corrosion from visual inspection. The amount of corrosion described could be quantified and documented by the use of photos or sketches. For precise measurements of local corrosion penetration by pitting corrosion caused, for instance, numerous kinds of optical or mechanical measuring instruments may be used.

b) **Weight loss measurement (ASTM G1)**: In this technique, the samples are tracked for the variation of its own weight loss after cleaning the specimen. Also based on the weight loss and surface area of the specimen over a specified time the corrosion rate (mm/year) can be determined. (Seica, 2000; and Rajani, 1996)
c) **Radiography, ultrasonic and acoustic testing:** These assessments are based on various types of waves and consequently identify any types of breaks or deformities flaws within the testing samples and pipes. There are many restrictions in identifying just the bodily deformities or breaks in certain kind of alignments. These can't be used-to identify deterioration problems which are mainly chemical and /or biological and result in a lack of physical strength in the place.
d) **Liquid penetration and leak detection methods:** This method is used to detect surface cracks where the surface is coated with specific liquids (paraffin), and penetration is analyzed which indicates the existence of cracks.
e) **Electrical methods:** In this method, standard electrodes are used to measure the potential drop over the period of time to determine the corrosion. Also four probe direct current method is being used to measure the change in resistance as an outcome of the corrosion and cracks. This really is helpful in finding the crack and flaws as a consequence of corrosion in the metal surface.
f) **Electrochemical methods (ASTM G3):** Electrochemical processes evaluate the extent of damage to the metal in corrosive. Various electrochemical procedures like the Linear Polarization Resistance (LPR) process, Electrochemical Impedance Spectroscopy (EIS) procedure, and Electrochemical Noise measurements are used to monitor the corrosion rate of the metallic surface. Polarization measurements are being used to investigation a variety of electrochemical phenomena (Mirtaheri et al. 2005).

Major Issues and Concerns

Corrosion of materials including steel will not only affect the exposed surfaces but also the integrity of the bulk material. On the surface corrosion will be two dimensions (2D). Within the bulk steel, corrosion will be in all directions (3 dimensional-3D) and also not homogenous and hence changes have to be quantified point-to-point or section-by-section to better understand the corrosion processes. Corrosion of steel is a bio-chemo-physical-stress-thermo (BCPST) induced parallel and/or series processes (representing varying environments and usage) and the corrosion and degradation are very much time depended. The physical properties will represent the material composition, density, shape of the sample and surface conditions. The stresses can be multi axial static and fatigue loading. Over the past 200 years several corrosion measurement methods have been developed to measure the changes in weight, rate of thickness loss, color changes, critical current density, linear polarization resistance,

potential difference, ultrasonic wave travel time and many more. Unfortunately none of these methods clearly separate the surface corrosion from the bulk corrosion in all types of materials including steel.

Objective

The overall objective was to verify the sensitivity of the new nondestructive two probe alternative current method to detection and quantify the surface and bulk corrosion using steel specimens. The specific objectives were as follows:

i. Using the newly developed characterization Vipulanandan Impedance Corrosion Model identify the electrical properties (resisitivity (resistance), permittivity (capacitance), permeability (inductance)) of the steel related to corrosion.

ii. Investigate the surface and bulk corrosion development with time for steel specimens placed in 3.5% salt solution and quantify the surface and bulk corrosion along the length of the steel specimens.

iii. Compare the standard test results such as weight loss, potential drop and visual inspection due to corrosion with the new nondestructive test method where changes in the electrical properties used to quantify the corrosion.

Materials and Methods

Steel Plates

Corrosion of carbon steel, ASTM A36-14, was used for this study. Based on the manufacturer's data sheet, the iron content varied from 98.8% to 99.3% with a carbon content of 0.18%. For the weight loss and potential difference study the samples uses were 3 inches in length. For the electrical characterization of corrosion, the steel bars used were 30 inches in length 1.2 in in width and 0.16 in thickness. The specific gravity of the carbon steel was 7.86 (ASTM G1-03).

Salt Solution

Both, 3.5% sodium chloride (NaCl) salt solution is representing the sea water and for the accelerated test, 10% sodium chloride (NaCl) solution is representing the hydraulic fracturing fluids with high salt contents, were used. The steel specimens were placed in the selected solution in a plastic container for the entire duration of testing.

Theory and Concepts

VIPULANANDAN IMPEDANCE MODEL (Vipulanandan et al. 2013)

Equivalent Circuit

It is importnat clearly identify the electrical properties (resisitivity (representing

resisitance R), permitivity (representing capacitance, C) and permeabilty (representing inductance, L)) of the material that will represnt the corroding material. Identification of the most appropriate equivalent circuit to represent the electrical properties of a material is essential to further understand its properties and the changes due to corosion.In the literature, there are data on impedance frequency responses of materials but there no clear represeantion of the electrical properties that influence the response.

In this study, different possible equivalent circuits were analyzed to find an appropriate equivalent circuit to represent the corroding steel with two probe monitoring.

CASE 1: General Bulk Material – Resistance and Capacitor

In the equivalent circuit for CASE 1 (Fig. 1(a)), the contacts were connected in series, and both the contacts and the bulk material were represented using a capacitor and a resistor connected in parallel (Fig. 1(a)).

In the equivalent circuit for CASE 1, R_b and C_b are resistance and capacitance of the bulk material, respectively and R_c and C_c are resistance and capacitance of the contacts, respectively. Both contacts are represented with the same resistance (R_c) and capacitance (C_c) as they are identical.Total impedance of the equivalent circuit for Case 1 (Z_1) can be represented as follows:

$$Z_1(\sigma) = \frac{R_b(\sigma)}{1+\omega^2 R_b^2 C_b^2} + \frac{2R_c(\sigma)}{1+\omega^2 R_c^2 C_c^2} - j\left\{\frac{2\omega R_c^2 C_c(\sigma)}{1+\omega^2 R_c^2 C_c^2} + \frac{\omega R_b^2 C_b(\sigma)}{1+\omega^2 R_b^2 C_b^2}\right\}, \quad (1)$$

where ω is the angular frequency of the applied signal. When the frequency of the applied signal was very low, $\omega \rightarrow 0$, $Z_1 = R_b + 2R_c$, and when it is very high, $\omega \rightarrow \infty$, $Z_1 = 0$.

CASE 2: Special Bulk Material - Resistance Only

In CASE 2 (Fig. 1(b)) , as a special case of CASE 1, the capacitance of the bulk material (C_b) was assumed to be negligible.

The total impedance of the equivalent circuit for CASE 2 (Z_2) is as follows:

$$Z_2(\sigma) = R_b(\sigma) + \frac{2R_c(\sigma)}{1+\omega^2 R_c^2 C_c^2} - j\frac{2\omega R_c^2 C_c(\sigma)}{1+\omega^2 R_c^2 C_c^2}. \quad (2)$$

When the frequency of the applied signal was very low, $\omega \rightarrow 0$, $Z_2 = R_b + 2R_c$, and when

it is very high, $\omega \rightarrow \infty$, $Z_2 = R_b$ (Fig. 2).

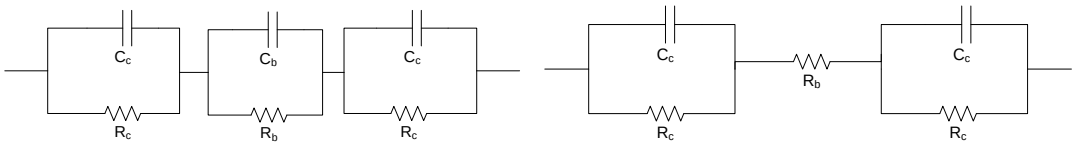

(a) **(b)**

Figure 1. Equivalent electrical circuits for (a) CASE 1 and (b) CASE 2

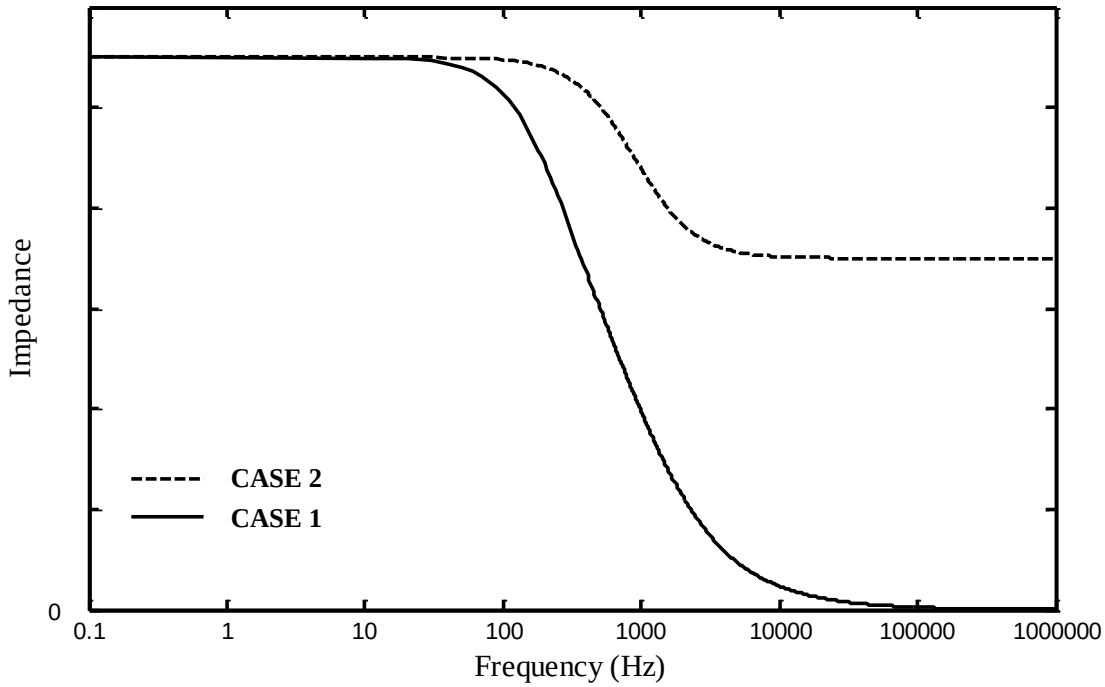

Figure 2. Comparison of typical responses of equivalent circuits for CASE 1 and CASE 2

Results, Verification and Discussion

1. Method 1: Weight Loss Study (ASTM G1-03)

Steel samples with a initial length of 3.00 in. and a width of 1.20 in. and thickness of 0.16 in. were used for this experiment. Three specimens were tested. Specimens were placed in 10% sodium chloride solution and tested regularly by cleaning

the specimens and measuring the weight and dimensions. In the initial average weight was 812.1 g and it reduced to 803.6 g in one year. The specimens were cleaned using mechanical tools and with were measure after 2, 3, 6 and 12 months. The percentage weight change was related to the testing time (t) (Fig. 3) using the Vipulanandan correlation model (Eqn. (3)) (Vipulanandan et al. 2016) and the relationship is as follows:

$$\frac{\Delta W \times 100}{W} = \frac{t}{A+Bt} \quad (3)$$

Where W was the initial weight of the specimen and □W was the weight change. The weight change after one year was 1.05%. The model predicted the test results very well with a coefficient of verification (R^2) of 0.99. The parameter A was 4.98 months and parameter B was 0.53. So the ultimate predicted weight change will be 1.88% when the time of exposure is very large (time is infinity).

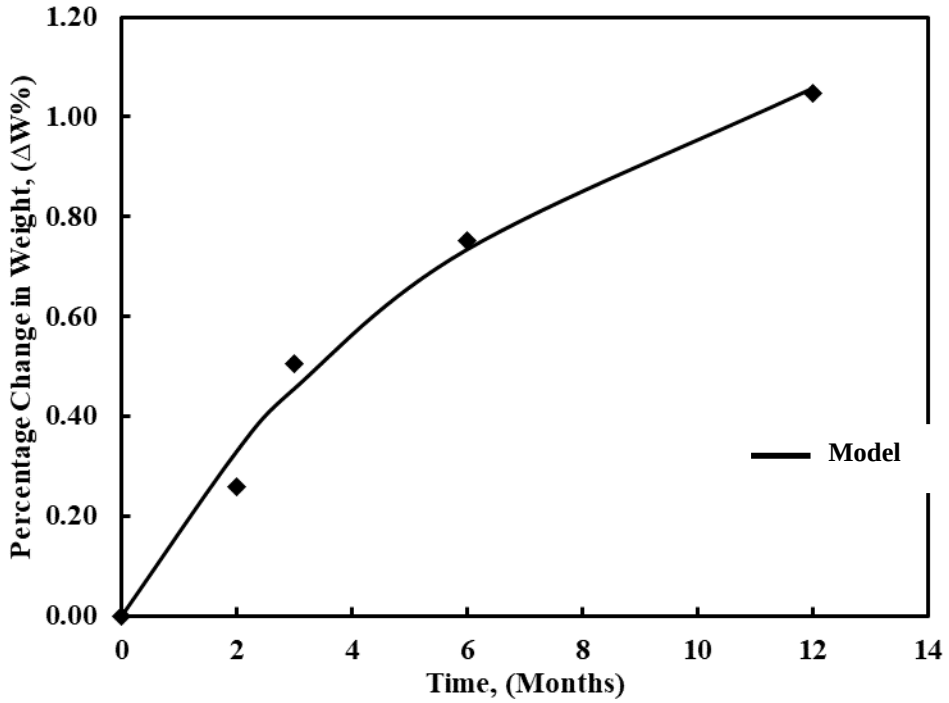

Figure 3. Variation of Average Weight Loss for the Corroding Specimens with Time in 10% NaCl Solution

Using the ASTM G1-03 standard the corrosion rate (mm/year) was determined using the following relationship:

$$Corrosion\ Rate = \frac{K \times \Delta W}{Area \times Time\ (hours) \times Density} \quad (4)$$

The carbon steel density was 7.86 g/cm^3 and the K parameter for estimating the corrosion rate in mm/year was 8.76x10^4. The estimate corrosion rate using Eqn. (4) was 1.54 mm/year or 0.06 inches/year in 10% NaCl solution. The estimated rate of corrosion was about three times the corrosion rated reported for sea water (3.5% NaCl) in the literature and hence the results are comparable.

2. Method 2: Potential Difference Study (ASTM G82)

The potential differences between corroding steel in 1 M NaCl solution and a standard calomel electrode (SCE) was monitored for two years using a multimeter (Fig. 4). The spacing between the corroding steel and SEC was about 1 inch. The variation of the potential difference with time is shown in Fig. 4. The initial potential difference was 0.68 V and it decreased to 0.791 V in two year, a 15% reduction. Hence the percentage change in the voltage was much higher than the percentage change in weight.

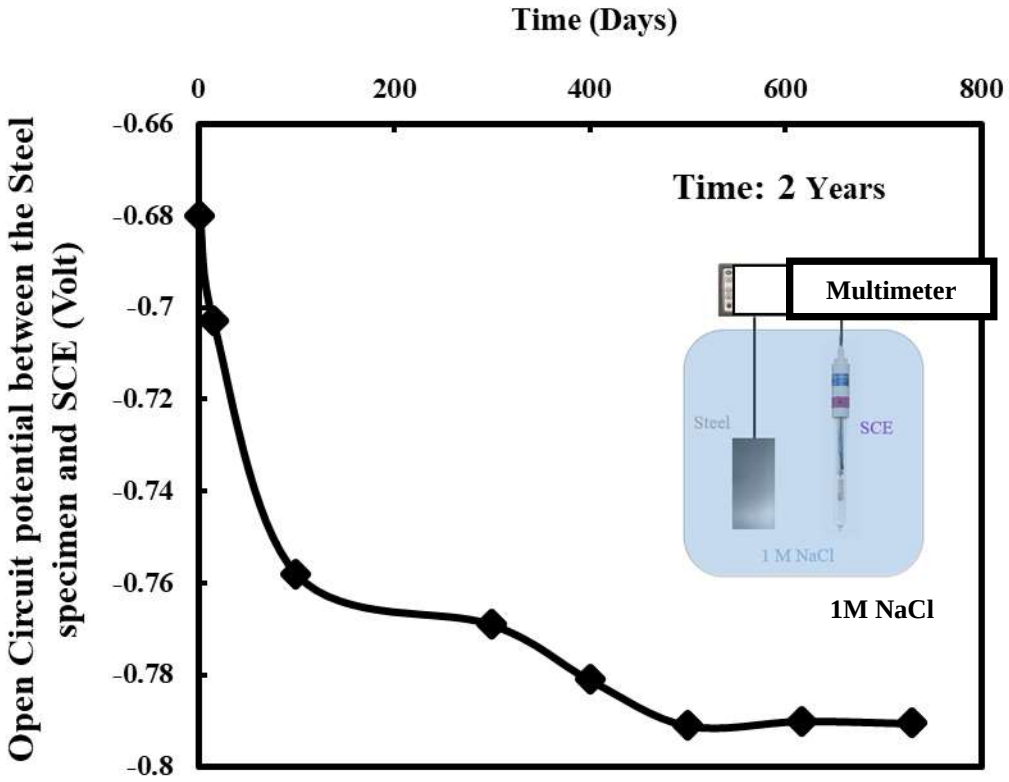

Figure 4. Potential Difference between Corroding Steel Specimen in 1 M NaCl Solution and and Standard Calomel Electrode (SCE)

3. Method 3: Visual Inspection Study

The 30 in long steel specimens placed in 3.5% NaCl solution were visually inspected on a regular basis. Images of the corroded steel surfaces long the length in three locations are shown in Fig. 5 and the corrosion was not uniform and it changed from point to point. As shown in Fig. 5, Locations #2 and #3 showed more corrosion than Location #1. For the new NDT method Locations #1 and #2 were used as the Contacts #1 and #2 respectively.

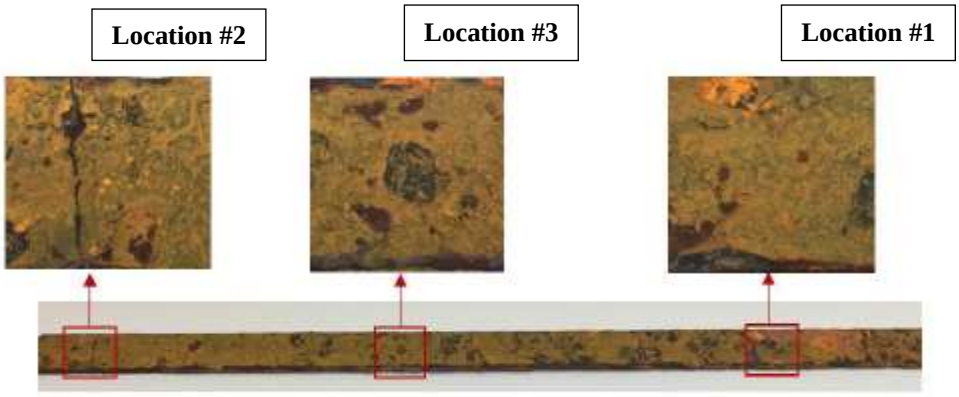

Figure 5. Visual Inspection of Surface Corrosion of Steel Specimen Corroded in 3.5 % NaCl solution for a testing period of 1 Year

4. Method 4: New Nondestructive Two Probe Resistivity Study (U.S. Patent 2020)

The 30 in long steel specimens placed in 3.5% NaCl solution were tested regularly to detect and quantify corrosion using the two-probe alternative current method (Fig. 6). The alternative current frequency was varied from 20 Hz to 300 kHz.

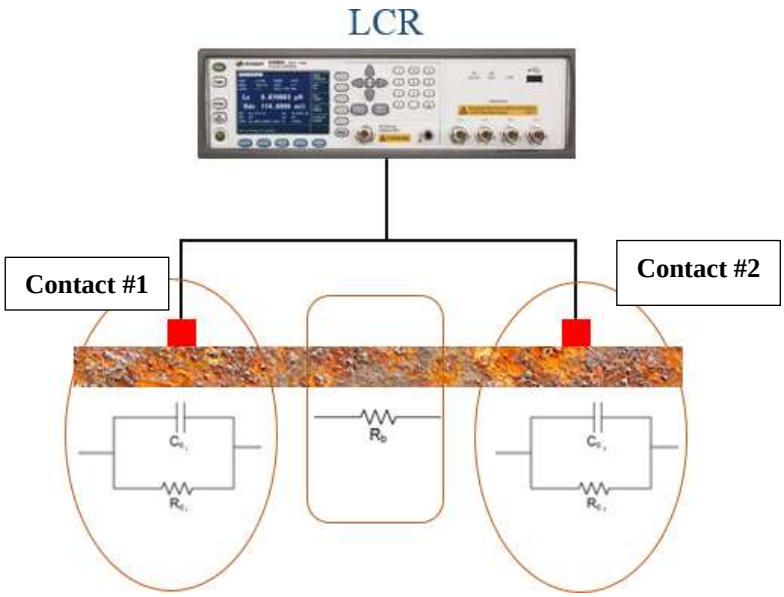

Figure 6. Testing Configuration for the New NDT Resistivity Method

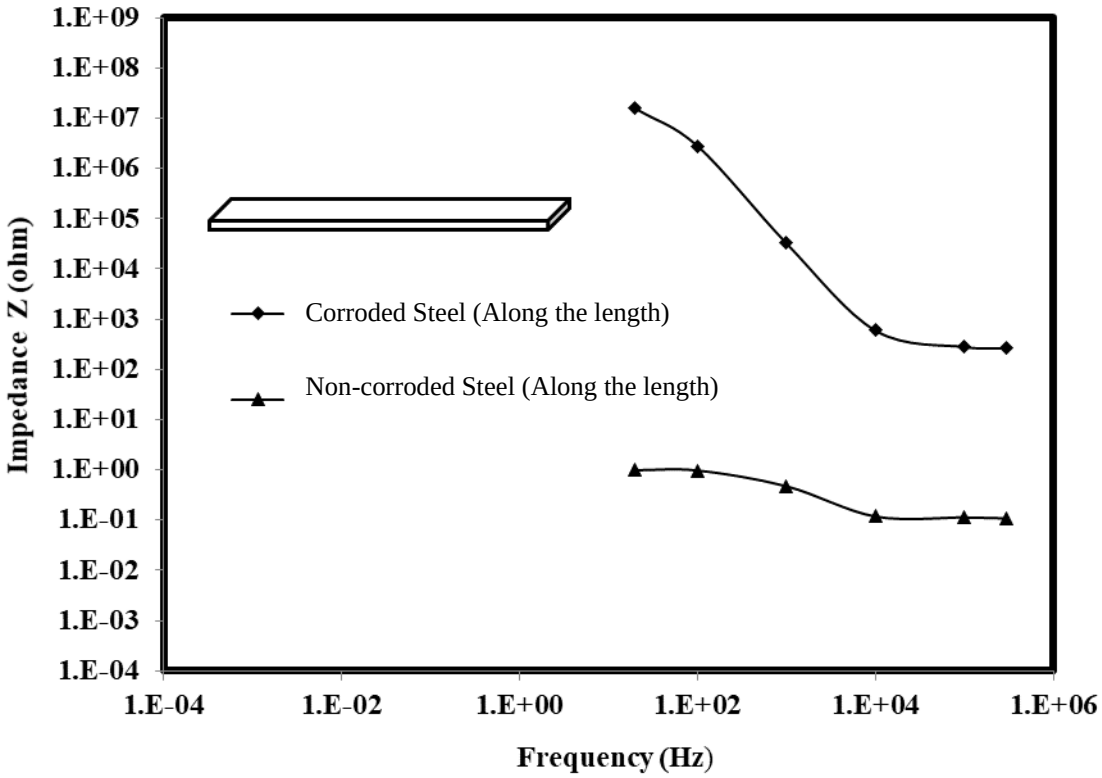

Figure 7. Impedance – Frequency Responses for Non corroded and Corroded Steel

The responses for both non-corroded and corroded steel were CASE 2 as shown in Fig.7. This is the identification of the impedance circuit for the current corrosion study.

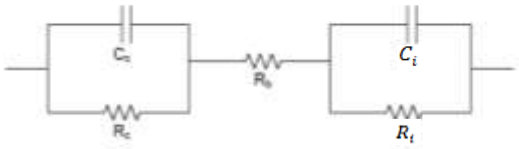

CASE 2 -Corrosion

$$Z = R_b + \frac{R_c}{1+\omega^2 {R_c}^2 {C_c}^2} + \frac{R_i}{1+\omega^2 {R_i}^2 {C_i}^2} - j\left(\frac{\omega {R_c}^2 C_c}{1+\omega^2 {R_c}^2 {C_c}^2} + \frac{\omega {R_i}^2 C_i}{1+\omega^2 {R_i}^2 {C_i}^2}\right) \quad (5)$$

Figure 8. Vipulanandan Impedance Corrosion Model

Based on the impedance-frequency response of the steel, CASE 2 equivalent circuit was

used to determine the contact electrical resistances with time (t) at each contact locations (R_c (t) and R_i(t)) and contact capacitances (C_c(t) and C_i(t)) on the surface of the steel specimen. During the impedance characterization at least 15 data were collected for each test and the data was used to determine the five unknowns (Rb, Rc, Ri, Cc, Ci) in the Eqn. (5) using the least square method.

The resistance (R) and capacitance (C) for a material between two points of measurements is defined as:

$$R = \rho K = \rho \frac{L}{A} \quad (6)$$

$$C = \epsilon \frac{A}{L} \quad (7)$$

where A = cross-sectional area, L = distance between the two probes, ρ = resistivity of the material, ϵ = absolute permittivity of the material

The product of equations given in (6) and (7) results as

$$RC = \rho\epsilon. \quad (8)$$

Since ρ and ϵ in equations (6) and (7) are material properties, RC at the point of contact is also material property (Eqn. (8)) and will be referred as electrical corrosion index. This parameter can be used in characterizing the surface corrosion at each point.

The electrical resistivity (ρ) of the bulk steel specimen was determined from the R_b measured along the length of specimen between the two points of contact and using the Eqn. (6) the following relationships was developed (Vipulanandan et al. 2013 & 2018):

$$\frac{\Delta \rho(t)}{\rho_0} = \frac{\Delta R(t)}{R_0} \quad (9)$$

$$\rho(t) = \rho_0 + \Delta\rho(t) \quad (10)$$

Where the initial resistivity of non-corroded steel ρ_0 =1.59 E^{-07} Ωm (Douglas, 1991) and R_o is the initial resistance measure and ΔR(t) is the change in resistance (R_b(t) –R_o). The Δρ is the change in resistivity.

4a. Bulk Corrosion

The impedance-frequency measurements were performed on a weekly basis for 500 days. The frequency range used was from 20 Hz to 300 kHz. The $R_b(t)$ increased non-linearly with time as shown in Fig. 9. After 500 days of corrosion, the bulk $R_b(t)$ along the length of the corroded steel between Contact #1 (Location #1) and Contact #2 (Location #2) (2 feet apart, Fig 5) increased from 0.131Ω to 5810 Ω which showed a change of 44,351 (4,435,100 %).

The resistivity of the corroding steel changed from 1.59 $x10^{-7}$ Ωm to 7.05 $x10^{-3}$ Ωm along the 2 feet length during the testing period of 500 days (Fig. 10), the change is 44,340 times (4,434,000%) which indicated the resistivity was a highly sensing material property to represent the corrosion level within the bulk steel. The change in the electrical resistivity, a material property, is part of the corrosion of the steel, but could not be quantified by any other standard test methods.

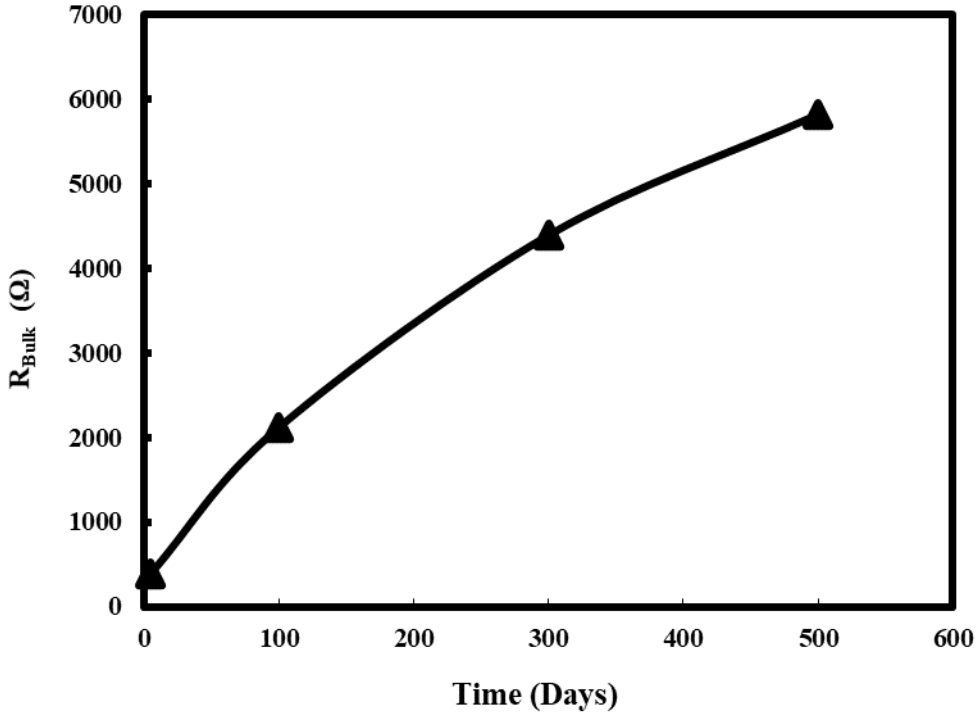

Figure 9. Variation of Bulk Resistance with Time in 3.5% Salt Solution (500 Days)

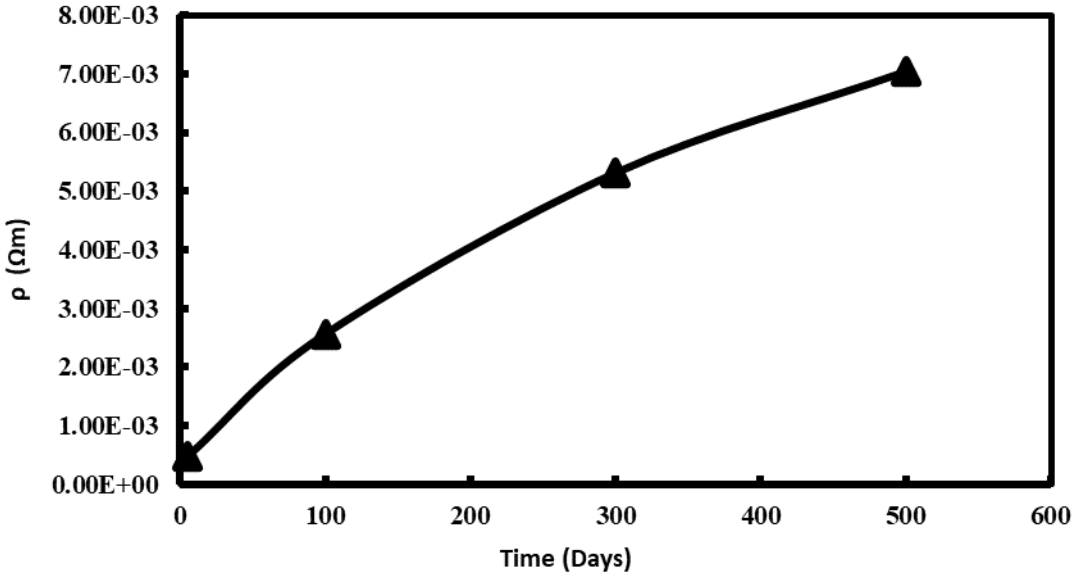

Figure 10. Variation of Electrical Resistivity of the Bulk Steel with Time in 3.5% NaCl Solution

4b. Surface Corrosion

Contact Resistance (R_c and R_i)

Based on the impedance-frequency measurements performed on a weekly basis the Contact #1 resistance $R_c(t)$ increased non-linearly with time as shown in Fig. 11. The Contact #1 resistance increased from 0.07 Ω to 7322 Ω during the testing period of 500 days, indicating an increase of 104,600 times.

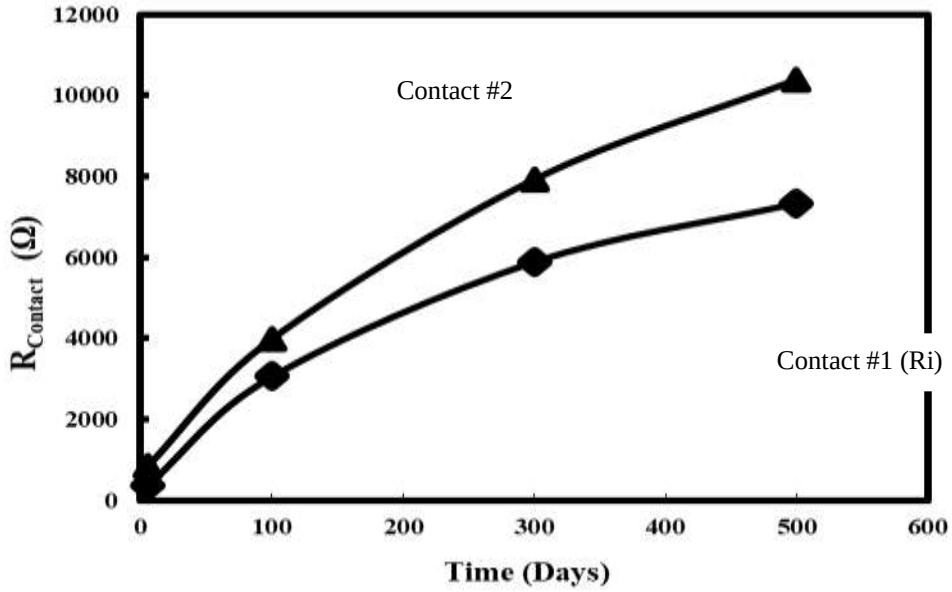

Figure 11. Variation of Contact Resistances with Time for the Corroding Steel

Specimen in 3.5 % NaCl Solution

The variation of Contact #2 resistance (R_i) is also shown in Fig. 11 for the testing time period of 500 days. The contact resistance (R_i) increased with time from 0.07 Ω to 10388 Ω in a testing period of 500 days, 148,400 times. The percentage increase was about 42% higher than Contact #1 indicating that the steel surface corrosion was not uniform and at Contact #2 the corrosion was higher than Contact #1, justify the visual observation in Fig. 5. This is another indicator of the uniqueness of the new test method for quantify corrosion.

Contact Capacitance (C_c and C_i)

The variation of capacitance at Contact #1 on the steel surface is shown Figure 12. The contact capacitance of Contact #1 decreased with increasing corrosion time, just the opposite of resistance. The capacitance value of the Contact #1 of the steel surface decreased from 1.58 E^{-09} F to 3.06 E^{-10} F during the testing period of 500 days, and it decreased by 80.6%.

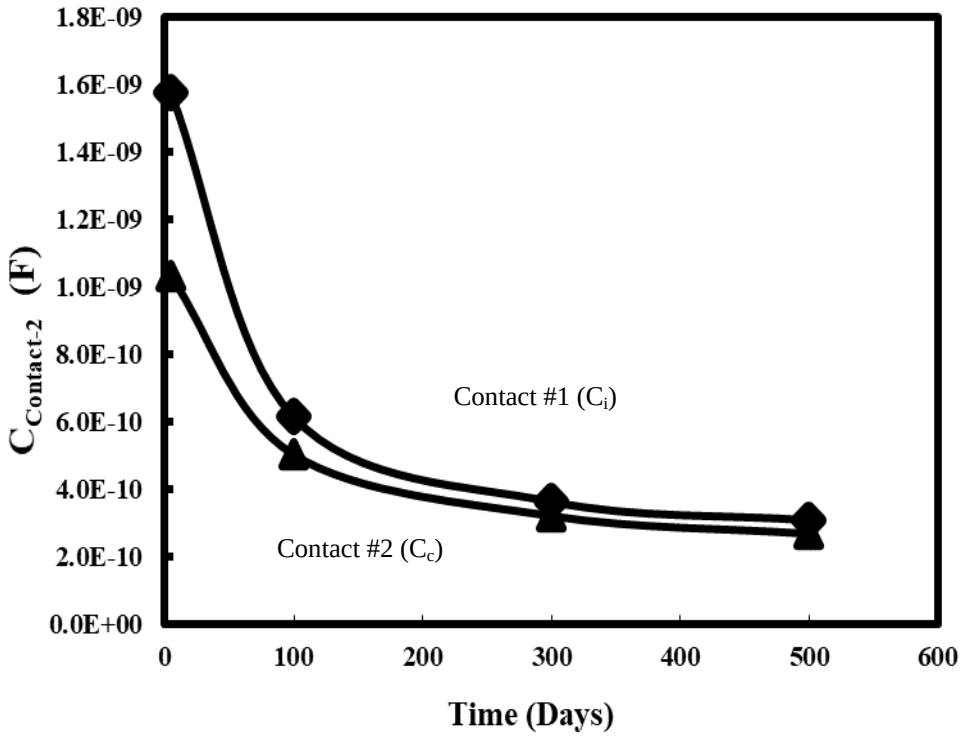

Figure 12. Contact #1 Capacitance of the Corroding Steel Specimen in 3.5 % NaCl Solution

The variation of capacitance at the Contact #2 on the steel surface (C_i) is shown in Figure 12. The capacitance of Contact #2 was lower than Contact #1. The contact capacitance of the Contact #2 decreased with increasing corrosion period. The capacitance reduced from 1.03 E^{-09} F to 2.67 E^{-10} F, a 74% decrease and the percentage change was lower than Contact #1.

Contact Corrosion Index (RC)

The variation of contact corrosion index, material property (R*C), for the corroding steel at Contact #1 in 3.5 % NaCl solution is shown in Figure 13. From the Fig.5, the rust material on the surface of the corroding steel increased with time. The R_CC_C at Contact #1 increased from 5.97 E^{-07} ΩF to 2.24 E^{-06} ΩF during the testing period of 500 days, 2.75-time (275%) increase.

The Contact #2 corrosion index parameter R_iC_i increased from 8.72E^{-07} ΩF to 2.77E^{-06} ΩF as shown in Fig. 13. The contact index parameter increased by 2.2 times (220%). The corrosion index parameter after 500 days of testing at Contact #2 was higher than Contact #1, by about 24%. The corrosion index clearly quantified the surface conditions at the measured two points, and the two points were not the same and also the visual inspection showed the difference on the surface.

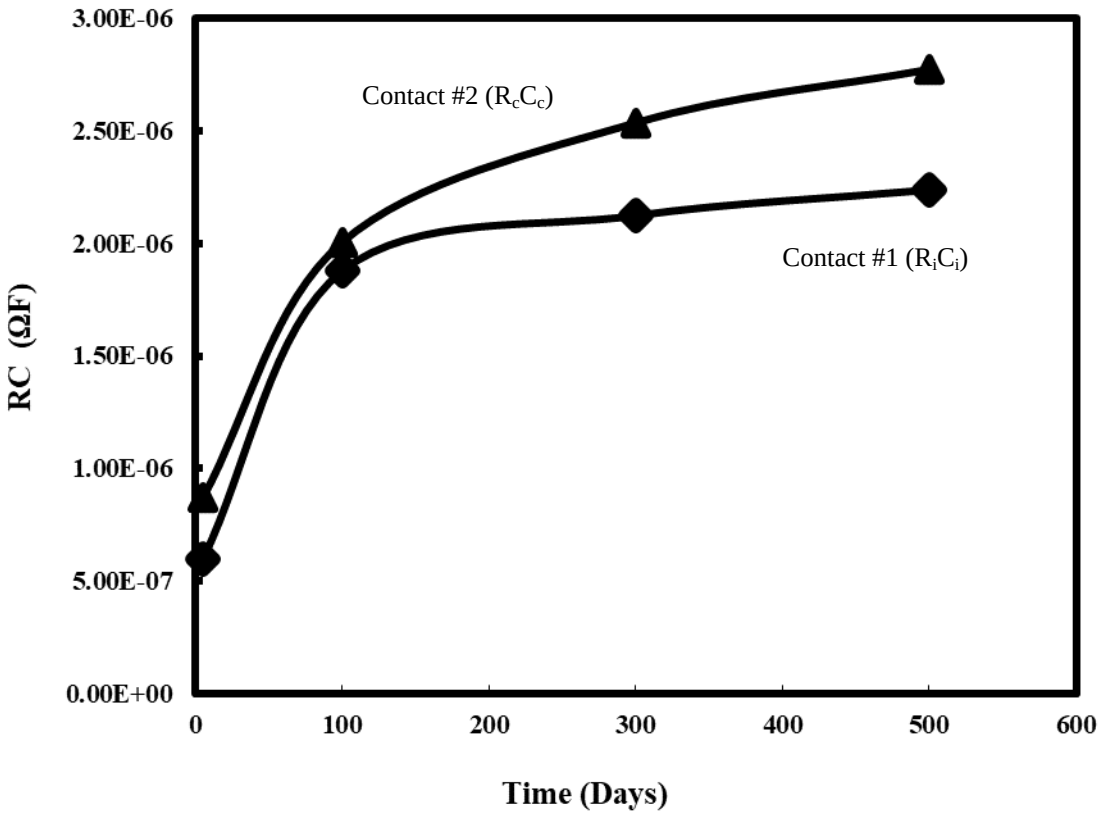

Figure 13. Corrosion Index Parameters for the Two Contact Locations on the Corroding Steel Surface in 3.5 % NaCl Solution

Conclusions

In this study the new nondestructive rapid detection and quantification of corrosion was verified and compared with some of the standard test methods using carbon steel. Base on this study following conclusions are advance:

1. The weight change in steel in 10% NaCl solution in one year was about 1%, and corrosion rate was 1.54 mm/year.
2. The potential reduction was in 1M NaCl solution was from -0.68 Volts to -0.791 Volts in two years about 15%.
3. The new nondestructive test separated the surface corrosion from bulk corrosion. The method clearly identified resistivity to be a highly sensing material property to characterize the bulk corrosion in steel. The bulk resistivity increase in corroding steel in 3.5% salt solution in 500 days was over 4,430,00%, much more sensitive than the weight loss method and potential difference methods.
4. Also, a new corrosion index was developed and verified to characterize and quantify the surface condition on the corroding steel. The corrosion was different at the two tested points and the visual observation verified it. The corrosion index increased in corroding steel in 3.5% salt solution in 500 days was over 200%.
5. Based on the material property changes, the surface corrosion was less than the bulk corrosion based on the new test method.

Acknowledgements

This study was supported by the Center for Innovative Grouting (CIGMAT) and the Texas Hurricane Center for Innovative Technology (THC-IT) at the University of Houston, Houston, Texas with the support from various industries.

References

1. ASTM A 36/A 36M – 04 Standard Specification for Carbon Structural Steel, Annual Book of ASTM Standards, Vol: 01.04, West Conshohocken, Philadelphia.
2. ASTM G1-03 (2017), “Standard Practice for Preparing, Cleaning, and Evaluating Corrosion Test Specimens”, ASTM Standards, Vol: 03.02, West Conshohocken, Philadelphia.
3. ASTM G4-01 (2014), “Standard Guide for Conducting Corrosion Tests in Field Applications”, ASTM Standards, Vol: 03.02; West Conshohocken, Philadelphia.
4. ASTM G31-72, “Standard Practice for Laboratory Immersion Corrosion Testing of Metals”, ASTM Standards, West Conshohocken, Philadelphia.
5. ASTM G82-98 (2014), “Standard Guide for Development and Use of Galvanic Corrosion Performance”, ASTM Standards, West Conshohocken, Philadelphia.
6. Chiew, S.P., Yu, Y. and Lee C.K. (2011) “Bonding failure of steel beams strength with FRP laminates-Part 1”, Journal of Constructional Steel Research 66, pp. 1047-1056.
7. Cheung, C.W.S. and Walsh, F.C. et al (1994) “Microbial Contributions to the Marine Corrosion of Steel Piling.” International Biodeterioration &

Biodegradation, 259-274.
8. Davis, J.R. (2000). “Corrosion: Understanding the Basics.", Vol.1, pp. 223-254.
9. Decker, J. B., Rollins, K. M. and Ellsworth, J. C. (2008). “Corrosion Rate Evaluation and Prediction for Pile Based on Long-Term Field Performance.” Geotechnical and Geoenvironmental Engineering, 341-351.
10. Evans, U.R. (1923), “The Mechaisms of the the So-Called Dry Corrosion of Metals,” Transaction of Faraday Society, Vol. 19, pp. 201-212.
11. Forrest, H.O., Roetheli, B.E. and Brown, R.H. (1931), Journal of Industrial and Engineering Chemistry, Vol. 23, pp. 650.
12. Hamdy, A.S., Shenawy, E.E. and Bitrar, T.E., (2006), “Electrochemical Impedance Spectroscopy Study of the Corrosion Behavior of Some Niobium Bearing Stainless Steels in 3.5% NaCl,” Int. J. Electrochem. Sci., 1, pp. 171-180.
13. Hilbert, L.R. (2006). “Monitoring corrosion rates and localised corrosion in low conductivity water,” Corrosion Science, Vol. 48, No. 12, Dec 2006, pp. 3907-3923.
14. Jothilakshmi, N., Nanekar, P., Kain, V. (2013). “Assessment of Intergranular Corrosion Attack in Austenitic Stainless Steel Using Ultrasonic Measurements.” Corrosion.
15. Kamaitis, Z., (2008). “Modelling of Corrosion Protection for Reinforced Concrete Structures with Surface Coatings,” Journal of Civil Engineering and Management, 14(4), pp. 241–249
16. Krebs, L.A. (2003), “A Brief history of corrosion sensing methods.” Corrosion.
17. Kumar, A., Stephnson, L. D. (2002). “Accelerated Low Water Corrosion of Steel Piling in Seawater.” 30th International Navigation Congress.
18. Masadeh, S. (2005) “Electrochemical Impedance Spectroscopy Of Epoxy-Coated Steel” Journal of Minerals and Materials Characterization and Engineering, Vol. 4 No. 2, 2005, pp. 75-84.
19. McCafferty, E.(2010). “Introduction to Corrosion Science.” Vol.1, pp.21-23.
20. Mears, P.B. and Evans, U.R. (1935), “The Probability of Corrosion”. Transactions, Faraday Society, Vol. 30, pp. 527.
21. Mirtaheri, P. and Grimnes, S.(2005), “ Electrode Polarization Impedance in Weak NaCl Aqueous Solutions,” IEEE Transaction on Biomedical Engineering, Vol.52., No.12.
22. NACE International (NACE), 1440 South Creek Drive, Houston, Texas. (http://www.nace.org.)
23. Papavinasam, S. (2013). Corrosion Control in the Oil and Gas Industry, Gulf Professional Publishing (Vol.1, pp.5).
24. Popova, A., Sokolova, E. Raicheva, S. and Christov, M., (2004). “AC and DC study of the temperature effect on mild steel corrosion in acid media in the presence of benzimidazole derivatives,” Corrosion Science 45 (2003), pp. 33–58.
25. Rajani, B., Zhan, C., Kuraoka, S. “Pipe Soil Interaction Analysis of Joined Water Mains,” Canadian Geotechnical Journal. 33, 393-404, 1996.
26. Rebak, R.B., Xia, Z., Safruddin, R. and Szklarska-Smialowska, Z., (1995) "Electrochemical Processes Controlling SCC of Underground Pipelines", Paper No. 184, Paper presented at NACE International's Corrosion 95 Annual Conference.

27. Roberge, P. R., York San Francisco Washington, N., (1999). "Handbook of Corrosion Engineering." Vol.1, pp. 4.
28. Seica, M.V and Packer, J.A. (2000) "Mechanical Properties and Strength of Aged Cast Iron Pipes," Journal of materials in Civil Engineering, ISSN 0899-1561, 2000.
29. Swain, G.W. (1996) "OCE -4518 Protection of Marine Materials Class Notes", Florida Institute of Technology.
30. Townsend, H. E. (1996). "Behavior of Painted Steel and Aluminum Sheet in Laboratory" Corrosion.
31. U.S. Patent (2019) "Chemo-Thermo-Piezoresistive Highly Sensing Smart Cement with Integrated Real-Time Monitoring System" Inventor: C. Vipulanandan, Number 10,481,143 Awarded on November 19, 2019.
32. U.S. Patent (2020) "Rapid Detection and Quantification of Surface and Bulk Corrosion and Erosion in Metallic and Non-Metallic Materials with Integrated Monitoring System" Inventor: C. Vipulanandan, Number 10,690,586 Awarded on June 23, 2020.
33. Vipulanandan, C. and Liu, J.(2002) "Film Model for Coated Cement Concrete," Cement and Concrete Research, Vol. 32(4), pp. 1931-1936.
34. Vipulanandan, C. and Liu, J.(2002) "Glass-Fiber Mat Reinforced Epoxy Coating for Concrete in Sulfuric Acid Environment," Cement and Concrete Research, Vol. 32(2), pp. 205-210.
35. Vipulanandan, C., and Pan, D. (2012) "Repair Methods for Corroded Steel Piles" Proceedings, Deep Foundation Institute, CD, October 2012.
36. Vipulanandan, C. and Prashanth, P. (2013). "Impedance Spectroscopy Characterization of A Piezoresistive Structural Polymer Composite Bulk Sensor," Journal of Testing and Evaluation, Vol. 41, No. 6, pp. 898–904.
37. Vipulanandan, C., Ali, K., Basirat, B., A. Reddy, Amani, N., Mohammed, A. Dighe, S., Farzam, H. and W. J. Head (2016), "Field Test for Real Time Monitoring of Piezoresistive Smart Cement to Verify the Cementing Operations **,"** Offshore Technology Conference (OTC) 2016, OTC-27060-MS.
38. Vipulanandan, C., and Mohammed, A., (2016) "XRD and TGA, Swelling and Compacted Properties of Polymer treated Sulfate Contaminated CL Soil" Journal of Testing and Evaluation, Vol. 44, No. 6, pp. 1-16.
39. Vipulanandan, C., and Ali, K. (2018) "Smart Cement Grouts for Repairing Damaged Piezoresistive Cement and the Performances Predicted Using Vipulanandan Models" Journal of Civil Engineering Materials**,** American Society of Civil Engineers (ASCE), Vol. 30, No. 10, Article number 04018253.
40. Vipulanandan, C., and Amani, N. (2018) "Characterizing the Pulse Velocity and Electrical Resistivity Changes in Concrete with Piezoresistive Smart Cement Binder Using Vipulanandan Models" Construction and Building Materials, Vol. 175, pp. 519-530.
41. Vipulanandan, C., and Mohammed, A., (2018) "Smart Cement Compressive Piezoresistive Stress-Strain and Strength Behavior with Nano Silica Modification, Journal of Testing and Evaluation, ASTM, doi 10.1520/JTE 20170105.
42. Vipulanandan, C., Mohammed, A. and Ganpatye, A. (2018) "Smart Cement Performance Enhancement with NanoAl_2O_3 for Real Time Monitoring

Applications Using Vipulanandan Models," Offshore Technology Conference (OTC) 2018, OTC-28880-MS.
43. Whitney, W.R. (1903). "The Corrosion of Iron." J.Am.Chem.Soc.
44. Zaki, A. (2006). "Principles of Corrosion Engineering and Corrosion Control." Vol.1, pp.1.
45. Zhao, X. and Duan, J. et al (2007). "Effect of Sulfate-Reducing Bacteria on Corrosion Behavior of Mild Steel in Sea Mud". J. Mater. Sci. Technol., Vol. 23, pp 323-327.